Journal of Adhesion Science and Technology

ISSN: 0169-4243 (Print) 1568-5616 (Online) Journal homepage: http://www.tandfonline.com/loi/tast20

Adhesion performance of UV-cured semi-IPN structure acrylic pressure sensitive adhesives

Hyo-Sook Joo , Hyun-Sung Do , Young-Jun Park & Hyun-Joong Kim

To cite this article: Hyo-Sook Joo , Hyun-Sung Do , Young-Jun Park & Hyun-Joong Kim (2006) Adhesion performance of UV-cured semi-IPN structure acrylic pressure sensitive adhesives, Journal of Adhesion Science and Technology, 20:14, 1573-1594, DOI: 10.1163/156856106778884271

To link to this article: https://doi.org/10.1163/156856106778884271

Published online: 02 Apr 2012.

J. Adhesion Sci. Technol., Vol. 20, No. 14, pp. 1573–1594 (2006)

Also available online - www.brill.nl/jast

Adhesion performance of UV-cured semi-IPN structure acrylic pressure sensitive adhesives

HYO-SOOK JOO *, HYUN-SUNG DO, YOUNG-JUN PARK and HYUN-JOONG KIM †

Laboratory of Adhesion and Bio-Composites, Program in Environmental Materials Science, College of Agriculture and Life Sciences, Seoul National University, Seoul 151-921, South Korea

Received in final form 29 July 2006

Abstract—UV-curable solvent-free pressure sensitive adhesives (PSAs) are gaining importance in the area of adhesives because of increasing environmental concerns and the goal to reduce volatile organic compounds (VOCs) in work areas and consumption places. These PSAs have advantages such as low emission of VOCs, a solvent-free process, a fast producton rate at ambient temperature and only a modest requirement for operating space. In this study, UV-curable PSAs were investigated by measuring their adhesion performance in terms of probe tack, peel strength, shear adhesion failure temperature (SAFT) and holding power. PSAs were synthesized from 2-ethylhexyl acrylate (2-EHA), acrylic acid (AA) and vinyl acetate (VAc), using variations in AA concentration to control the glass transition temperature (T_g) of the prepared PSAs. In addition, two types of trifunctional monomers, trimethylolpropane triacrylate (TMPTA) and trimethylolpropane ethoxylated (6) triacrylate (TMPEOTA), which have different chain lengths, were used to form semi-interpenetrating polymer network (semi-IPN) structures after UV exposure. With increasing AA concentration in the PSAs, both the T_g and viscosity increased. Also, probe tack and SAFT increased, but peel strength decreased. After UV irradiation, probe tack decreased, and SAFT and peel strength increased as AA concentration increased in the PSAs. In most cases, cohesive failure changed to interfacial failure after UV exposure. Also, TMPTA increased the cohesion of PSAs; however, TMPEOTA affected the mobility of PSAs due to the different chain lengths of the two types of trifunctional monomer in a different way. The increase of TMPEOTA content diminished the cohesion of PSAs. Consequently, the adhesion performance of the PSAs was closely related to the T_g of the PSAs, and the two types of trifunctional monomer showed different adhesion performances.

Keywords: UV-curable PSA; semi-IPN; acrylic acid; TMPTA; TMPEOTA.

*Current address: Advanced Material R&D, LG Chem, Ltd./Research Park.

†To whom correspondence should be addressed. Tel.: (82-2) 880-4784. Fax: (82-2) 873-2318. E-mail: hjokim@snu.ac.kr

1. INTRODUCTION

Pressure sensitive adhesives (PSAs) are viscoelastic materials that can adhere strongly to solid surfaces upon application of a light contact-pressure for a short contact-time. Their performance can be evaluated in terms of tack, peel strength and shear strength. The Pressure Sensitive Tape Council (PSTC) has defined PSAs as materials with aggressive and permanent tack [1]. PSAs are used not only in food packaging, clothing and wood-based composites, but also in the transportation, construction, medical and leisure industries.

Among the raw materials for producing PSAs, acrylics are most widely used, as they possess some superior properties compared to many other materials used for PSAs: they are transparent, colorless and are resistant to yellowing under sunlight and oxidation, due to their saturated structure. Acrylic PSAs are generally copolymerized with low glass transition temperature (low T_g) monomers for tackiness and with high T_g monomers for cohesive strength [2]. As the acrylic PSAs have a linear structure, they have inadequate thermomechanical stability; therefore, a crosslinking reaction is needed to increase their thermomechanical stability. The crosslinking reaction is induced by a crosslinker, crosslinkable monomers and multifunctional chemical compounds such as multifunctional isocyanates, polycarbodiimides, amino resins, multifunctional ethyleneimines and multifunctional acrylates. PSAs containing a crosslinker have a pot lifetime, which is the time span during which PSAs can be coated after the crosslinker is added [3–5]. In order to overcome the pot lifetime, UV-curing techniques can be used, because coated PSAs can be crosslinked by UV. The UV-curing techniques used in the PSA crosslinking process can be divided into UV-polymerization and UV-crosslinking methods. The UV-polymerization method involves an oligomer, reactive monomer, photoinitiator and other additives, and the UV-crosslinking method utilizes a mixture of prepolymer, reactive monomer and photoinitiator.

The adhesion performance of a UV-curable PSA can be varied by varying the UV dose, photoinitiator type, the T_g of the prepolymer, and the functionality, concentration and structure of the monomer. In particular, the T_g of the prepolymer can affect adhesion performance. Asahara *et al.* [6] have reported that the crosslinking reaction increased both the creep resistance and the T_g of the acrylic PSAs. Therefore, one can control the peel strength by controlling the degree of crosslinking, which, in turn, controls the wettabiltity of the PSAs. Czech [7] showed that as the molecular weight and UV exposure time increased, the tack and peel strength of UV crosslinked PSAs decreased and cohesion increased. Moreover, Decker *et al.* showed that multifunctional monomers were crosslinked by UV exposure, which then increased the shear resistance [8].

In this study, we prepared prepolymer, multifunctional monomer and photoinitiator blends as UV-curable PSAs. Specifically, the prepolymers were acrylic PSAs with linear structure with various T_g values and monomer structures. The purpose of UV irradiation was to form a semi-IPN structure from the PSA blend by crosslinking the blended multifunctional monomer. The UV-cured PSAs were evaluated in

terms of tack, peel adhesion, shear adhesion failure temperature (SAFT) and holding power as a function of the T_g of the prepolymer, the content and structure of the trifunctional monomer and the UV dose.

2. EXPERIMENTAL

2.1. Materials

2-Ethylhexyl acrylate (2-EHA, Junsei, Japan), acrylic acid (AA, Junsei, Japan) and vinyl acetate (VAc, Kanto, Japan) were used as received. Also, methanol (Samchun, South Korea) and ethyl acetate (Duksan, South Korea) were used as solvents. 2,2′-Azobisisobutyronitrile (AIBN, Daejung, South Korea) was used as the initiator without further purification. Trimethylolpropane triacrylate (TMPTA, Aekyung, South Korea) and trimethylolpropane ethoxylated (6) triacrylate (TMPEOTA, Miwon Commercial, South Korea) were used as trifunctional monomers. Figure 1 illustrates the structures of the trifunctional monomers. 2,2-Dimethoxy-1,2-diphenylethanone (Miwon Commercial, South Korea) was used as the photoinitiator.

2.2. Preparation of acrylic PSAs

The prepolymers were prepared by solution polymerization as 40% solids. The typical synthesis method was as follows. Various amounts of 2-EHA and AA, 10.5 g

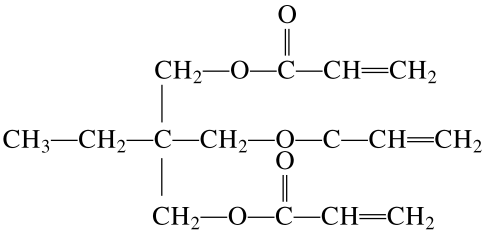

(a) TMPTA

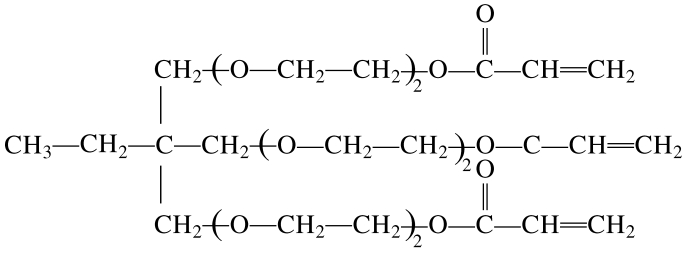

(b) TMPEOTA

Figure 1. Structures of the two types of trifunctional monomer used.

Table 1.
Blend ratio for the preparation of PSAs and characteristics of PSAs

	2-EHA (wt%)	VAc (wt%)	AA (wt%)	T_g (°C)[a]	Viscosity (cP)
PSA-A5	88	7	5	−49.8	16 000
PSA-A10	83	7	10	−46.9	30 000
PSA-A15	78	7	15	−43.5	65 000

[a] Measured by DSC.

VAc, 25 g methanol, 0.15 g AIBN and 50 g ethyl acetate (EAc) were mixed in a 500-ml four-neck flask equipped with a stirrer, a dropping funnel and a thermometer. This mixture was heated to 70°C with stirring. After the exothermic reaction was completed, the temperature was maintained for 30 min. A mixture of 100 g EAc and 0.3 g AIBN was added, and after 1 h, another mixture of 100 g EAc and 0.3 g AIBN was added. Finally, after 3 h, another 100 g EAc and 0.3 g AIBN was added, and after 1 h, the polymerization was stopped. The prepared prepolymer was used as a PSA. The compositions of the PSAs are listed in Table 1.

2.2.1. Viscosity. The viscosity of the prepared PSAs was measured using a Brookfield Viscometer (DV-II+) equipped with a RV-7 spindle. All measurements were performed at 20°C and 50% relative humidity.

2.2.2. Differential scanning calorimetry (DSC). The T_g was measured using a TA Instruments Q-1000 DSC. The samples were cooled to −80°C, heated to 150°C at a heating rate of 10°C/min for the first scan, immediately quenched to −80°C, and then kept at this temperature for 3 min. The samples were then reheated to 200°C at a heating rate of 5°C/min for the second scan. The T_g in this study was obtained from the second scan to assure reproducible thermograms free from thermal history effects.

2.3. Preparation of UV-curable PSAs

UV-curable PSAs were prepared by blending of synthesized PSAs, photoinitiator and trifunctional monomers. The amount of photoinitiator was 5 phr of trifunctional monomer. The UV-curable PSAs were coated onto a polyester film (PET, 50 μm, SKC, South Korea) using a bar coater No. 18 (wet thickness 41.1 μm), and were then dried at 70°C for 5 min. These UV-curable PSA films were cured using a UV-curing equipment with a 100-W high-pressure mercury lamp (main wavelength: 340 nm). The UV doses used were 0, 200, 600, 1000, 1400 and 1800 mJ/cm^2. The UV doses were measured with an IL 390C Light Bug UV radiometer (International Light, USA). The compositions of the UV-curable PSAs used in this study are given in Table 2.

Table 2.
Blend ratio of UV-curable PSAs

	TMPTA (wt%)	TMPEOTA (wt%)	Photoinitiator (phr)
Synthesized PSAs	10	—	5
	20	—	5
	30	—	5
	—	10	5
	—	20	5
	—	30	5

2.3.1. Gel fraction. The gel fraction of the PSAs blended with trifunctional monomers and the UV-cured PSAs was determined by soaking the samples in toluene for 1 day at 50°C. The sample amounts were about 5 g. In addition, the insoluble part of the PSAs was removed by filtration and dried at 50°C to a constant weight. The gel fraction was calculated by the following equation:

$$\text{gel fraction } (\%) = (W_1/W_0) \times 100,$$

where W_0 is the weight before filtration and W_1 is the weight after filtration.

2.4. Adhesion properties

2.4.1. Probe tack. We performed probe tests using Stable Micro Systems TA-XT2i texture analyzer (UK). A typical probe test can be divided into three stages: approach to the surface of PSA, contact and separation from the surface of PSA. The probe was moved at a rate of 0.5 mm/s, maintained on the PSA surface for 1 s under a constant force of 100 g/cm^2, and then debonding was carried out at a separation rate of 10 mm/s. In the debonding process, the probe tack result was recorded as the maximum debonding force. The probe used in this test was a standard, cylindrical, polished stainless steel probe supplied by Stable Micro Systems. The probe was cleaned with acetone after each test.

2.4.2. 180° peel strength. The specimens for the peel test were cut into 25 mm widths. After being removed from a siliconized release liner, each PSA film was attached to a stainless steel substrate, and then a 2 kg rubber roller was passed over it twice.

The peel strength was measured using Stable Micro Systems TA-XT2i texture analyzer (UK). The measurements were carried out at a crosshead speed of 300 mm/min at 20°C, based on ASTM D3330.

2.4.3. Shear adhesion failure temperature (SAFT). Each PSA sample was attached to a stainless steel substrate with a bonding area of 25 × 25 mm^2, and a 2 kg rubber roller was pressed onto the PSA sample once. The samples were hung

in the oven, and then a weight of 1 kg was hung at the end of each sample. The oven was heated from 25°C to 150°C at a heating rate of 0.4°C/min.

2.4.4. Holding power. PSA sample was pressed onto a stainless steel substrate with a bonding area of 25 × 25 mm^2 by using one pass of a 2-kg rubber roller. The samples were hung in the oven at 130°C, and then a weight of 1 kg was hung at the end of each sample. Break time, i.e., the time to separate from the stainless steel adherend, was measured.

3. RESULTS AND DISCUSSION

3.1. Preparation of acrylic PSAs

In this study, PSAs with varying amounts of AA were observed, and the expected effects of AA addition were good adhesion to different substrates, especially to metallic substrates; enhancement of cohesion; and increased viscosity [9].

3.1.1. Viscosity. Viscosity influences the wettability of PSAs on the substrates, so it has an important meaning for PSAs. For example, hot-melt adhesives need to be heated until melted for use. Heated adhesives have a low viscosity, so they wet the substrates. Solvent-based adhesives should be as liquid as possible so that they may 'wet' the surfaces thoroughly [6].

The viscosities of PSA-A5, PSA-A10 and PSA-A15 samples prepared are listed in Table 1. Although the prepared PSAs have linear structure, the hydrogen in the carboxylic group of PSAs is linked *via* a hydrogen bond. It looks that viscosity increased with increasing AA concentration due to this hydrogen bond which increased cohesion of PSAs. Similary, Li and Kwak [10] reported that the partial ionization of the AA group leads to strong interpolymer hydrogen bonding which, in turn, promotes interpolymer hydrophobic association, resulting in a large increase in solution viscosity.

3.1.2. Differential scanning calorimetry (DSC). The T_g is a major factor in selecting the comonomer for a PSA, and it is related to adhesion properties. In order to achieve good tack, it may be necessary to increase the content of soft acrylic monomer. For example, 2-EHA and butyl acrylate (BA) are most commonly used for reducing the T_g [6].

The T_g's values of PSA-A5, PSA-A10, and PSA-A15 are listed in Table 1. The T_g of the PSAs increased with increasing AA concentration, because AA has the highest T_g among the monomers used in this study. Similar results were reported by Kim and other researchers [11, 12]. They reported that the T_g of the co-polymers of AA and 2-EHA increased with increasing AA concentration.

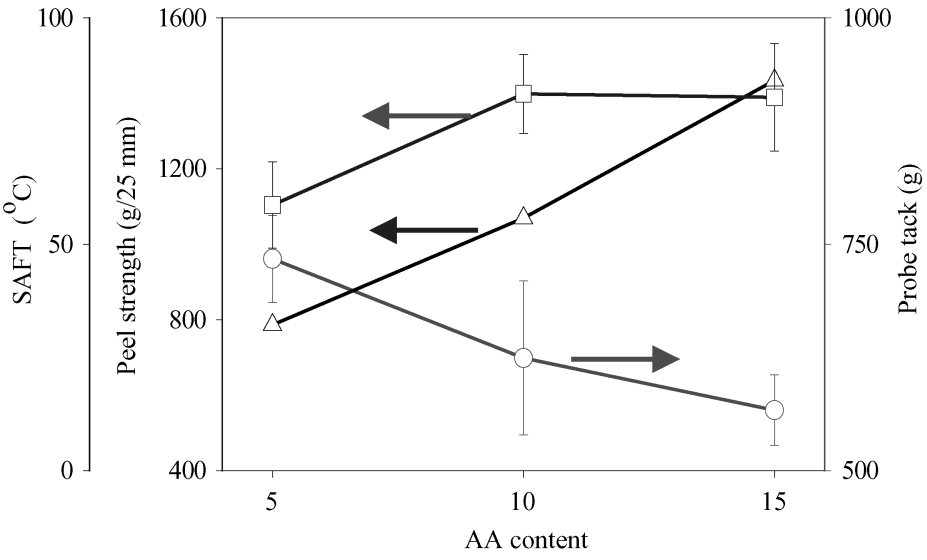

Figure 2. Adhesion properties: probe tack (–○–), peel strength (–□–) and SAFT (–△–) of PSAs with variation in AA content.

3.1.3. Performance of PSAs. The PSA performance was evaluated in terms of probe tack, peel strength and shear adhesion failure temperature (SAFT). These results are shown in Fig. 2.

Probe tack values decreased from PSA-A5 to PSA-A15 because PSA-A5 has a lower T_g and a lower viscosity than the other two PSAs. Zosel [9] showed that the maximum tack value was observed at a temperature which was the sum of the T_g of PSA and 50°C, and a rapid increase of adhesion energy and change of failure mode with temperature was shown. In this study, it was observed that tack decreased with increasing T_g at ambient temperature. Change from cohesive failure to interfacial failure was observed. The increase of AA concentration increases the T_g of PSAs because of the higher T_g of AA than other monomers. Therefore, the increase in the T_g changes the failure mode and eliminates fibrillation [13].

Peel strength slightly increased as AA concentration increased, although PSA-A10 and PSA-A15 showed somewhat similar peel strengths. These results can be explained, since the increase of AA concentration affected the viscosity and cohesive strength of synthesized PSA because of hydrogen bond formation. Therefore, the peel strength of PSAs increased with AA concentration. The T_g of a PSA has a pronounced effect on SAFT. Therefore, PSA-A15, which has the highest T_g, displays the highest SAFT among the three PSAs. In addition, PSA-A10 has a lower SAFT than PSA-A15 and a higher SAFT than PSA-A5. Therefore, an increase in SAFT is associated with an increase in the T_g of the PSA, and the T_g of the PSA is influenced by its AA concentration. Tobing and Klein [14] reported that increased T_g led to higher shear holding power. Therefore, to improve shear holding power, acrylic PSAs, in general, contain high T_g copolymers such as methyl ethyl acrylate,

methyl acrylate, and VAc. However, these copolymers also reduce both the peel strength and tack.

Consequently, the increase of the T_g raised the SAFT by sacrificing the tack. Also, all PSA samples showed cohesive failure when the peel strength and SAFT tests were performed because the synthesized PSAs are linear copolymers without crosslinking, which have low cohesive strength, although AA, a polar monomer, increased the cohesive strength and improved the interaction with the substrate [15].

3.2. UV curing of PSAs

PSAs were blended with trifunctional monomers TMPTA and TMPEOTA and a photoinitiator, and then the PSA blends were coated onto PET films. The PSA films were dried and cured by UV irradiation.

Before UV irradiation, PSAs are linear in structure, and their surfaces are soft. Although the trifunctional monomers have low molecular weights, trifunctional monomers in PSAs can be photopolymerized after UV exposure. Therefore, after UV irradiation, UV-curable PSAs can form semi-IPN structures, as illustrated in Fig. 3. Also, the surface of UV-cured PSAs becomes hard.

3.2.1. Gel fraction. Gel fraction can be determined by measuring the insoluble part of a PSA, such as crosslinked or network polymers. These insoluble polymers are only swollen when in contact with solvents. However, other parts, such as linear or branched polymers, are soluble. In this study, the soluble linear polymer, or PSA polymer, was turned into an insoluble three-dimensional network polymer of

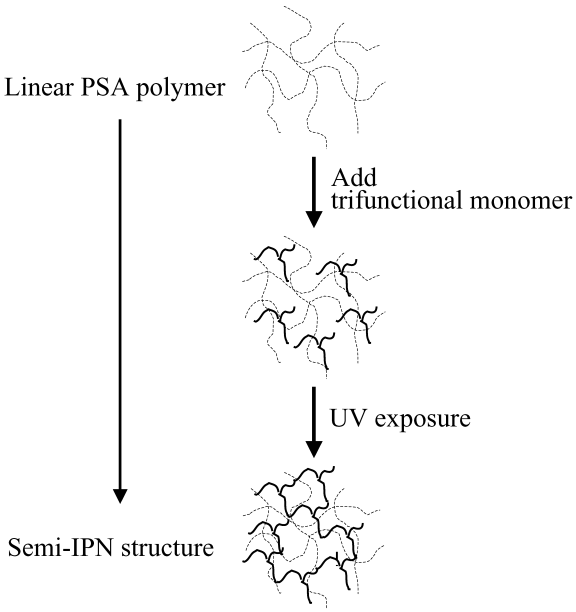

Figure 3. Process of producing semi-IPN structure in UV-cured PSAs.

infinite molecular weight and semi-IPN structure by photopolymerization using the trifunctional monomers TMPTA and TMPEOTA.

Table 3 shows the gel fraction of the UV-curable PSAs. After UV exposure, the gel fraction was dramatically increased. This increment is caused by crosslinking of trifunctional monomers after UV exposure. In addition, the TMPTA blends show a higher gel fraction than the TMPEOTA blends. After UV exposure, TMPTA formed a tightly crosslinked semi-IPN structure in the linear structure of PSAs having different AA concentrations because of its short chain length. However, the long chain length of TMPEOTA disturbed the formation of a tight network after UV exposure. Moreover, the gel fraction increased as the AA concentration of the PSAs increased both before and after UV exposure.

The content of TMPTA has an effect on the gel fraction of PSA-A5 because TMPTA effectively crosslinks the linear structure of PSA-A5 with low cohesion. However, the content of TMPEOTA influences the gel fraction of PSA-A15, because TMPEOTA, having a long chain length, acts as a plasticizer in PSA-A15. The gel fraction for TMPTA in PSA-A15 is higher than that for TMPEOTA.

These results are evidence of crosslinking after UV exposure, and show the different effects of different trifunctional monomers in PSAs.

3.2.2. Probe tack. The probe tack results for the PSAs blended with TMPTA before and after UV exposure are shown in Fig. 4. Before UV exposure, the probe tack value decreased with increasing TMPTA content, because TMPTA acts as a plasticizer.

The probe tack values of the PSA-A5 and 10 wt% TMPTA blends gradually increased upon UV irradiation because the cured TMPTA no longer acts as a plasticizer. After UV irradiation TMPTA increases the cohesive strength of blended

Table 3.
Gel fraction (%) of UV-curable PSAs

	UV dose (mJ/cm^2)	TMPTA (wt%)			TMPEOTA (wt%)		
		10	20	30	10	20	30
PSA-A5	0	6.2	6.1	4.5	7.1	7.1	8.9
	200	81.2	85.6	88.1	80.6	80.9	79.6
	1000	85.9	93.2	92.1	81.7	78.7	80.4
	1800	88.2	92.5	93.7	81.7	83.1	80.4
PSA-A10	0	41.6	53.8	27.3	41.9	28.9	26.2
	200	89.3	91.7	91.2	76.4	74.1	74.5
	1000	93.6	93.3	95.6	77.8	77.2	83.3
	1800	91.8	94.1	96.8	80.1	84.3	84.9
PSA-A15	0	64.4	64.6	59.9	50.1	49.4	61.2
	200	84.9	92.0	92.7	68.4	73.8	87.2
	1000	91.4	96.0	95.9	75.4	83.7	89.3
	1800	92.4	96.5	96.4	82.4	86.8	93.6

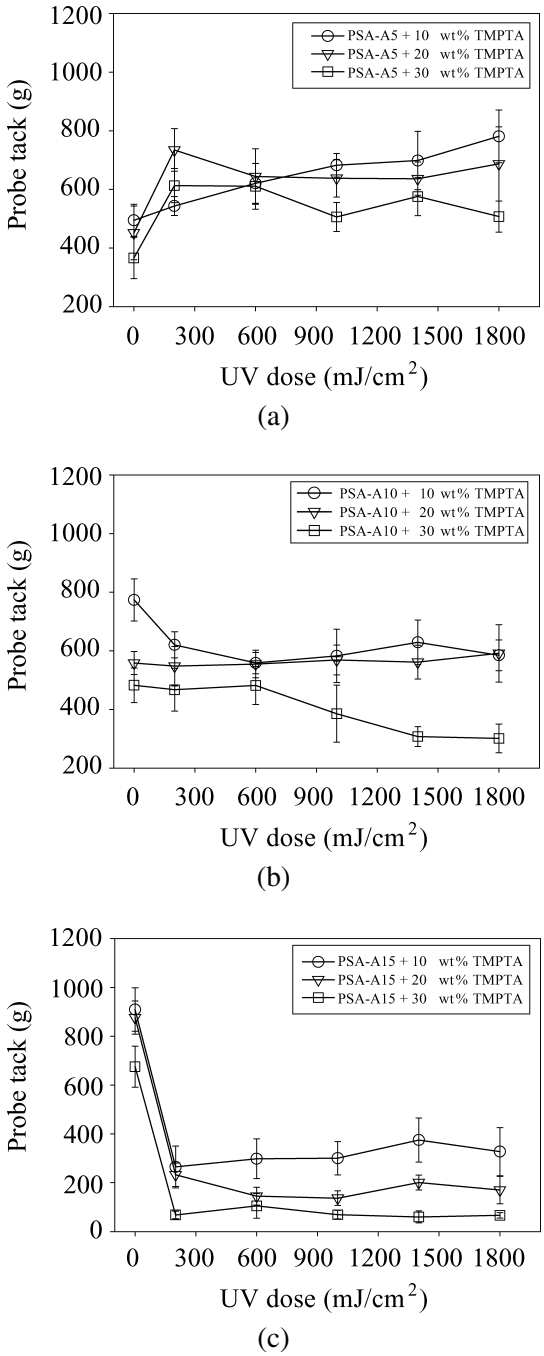

Figure 4. Probe tack of PSAs blended with (a) 10, (b) 20 and (c) 30 wt% TMPTA as a function of UV dose.

PSAs and forms a tightly crosslinked semi-IPN structure in PSAs after prolonged UV irradiation. In addition, the probe tack values of the PSA-A5 and 20 wt% TMPTA blends increased after 200 mJ/cm^2 of UV exposure, and then slightly decreased with higher UV irradiation. Moreover, the probe tack values of the PSA-A5 and 30 wt% TMPTA blend show a similar trend to that of the PSA-A5 and 20 wt% TMPTA blend. These results could be due to the decrease in PSA molecular mobility because of over-cured TMPTA, which could have a more tightly formed crosslinked semi-IPN structure, overly increased cohesion of PSAs and, consequently, decreased probe tack.

Moreover, after a UV dose of 200 mJ/cm^2, the probe tack values of the PSA-A10 and 10 wt% TMPTA blend decreased and remained constant, because after the TMPTA is cured, it can no longer act as a plasticizer, as shown in Fig. 4b. In addition, the probe tack of the PSA-A10 blended with 20 wt% TMPTA does not change upon UV irradiation because the uncured TMPTA acts like a plasticizer, but the cured TMPTA makes the surface of PSA-A10 hard and thus reduces probe tack. These different effects counterbalance each other, and thus there are no changes in probe tack. Furthermore, the PSA-A10 and 30 wt% TMPTA blend shows no change in probe tack value up to a UV dose of 600 mJ/cm^2. However, after a UV dose of 600 mJ/cm^2, the probe tack value is decreased because of cured TMPTA.

The probe tack value of PSA-A15 blended with TMPTA is drastically decreased after UV exposure, and then remains constant, as shown in Fig. 4c. The PSA-A15 with TMPTA blend shows low probe tack because the more tightly crosslinked structure of TMPTA elevated the cohesion of PSA-A15 blend and, thus, this blend loses its mobility. As a result, the probe tack values are reduced with increasing AA and TMPTA concentrations after UV exposure.

The probe tack value of PSA-A5 blended with TMPEOTA increased markedly after a UV dose of 200 mJ/cm^2, as shown in Fig. 5a. Also, we observed that fibrillation disappeared after UV exposure. This effect is due to the restricted mobility of the PSA polymer caused by the cured TMPEOTA. After a UV dose of 200 mJ/cm^2, the probe tack values of the PSA-A5 and TMPEOTA blends did not show significant changes, except for the PSA-A5 blended with 10 wt% TMPEOTA. The probe tack of the PSA-A5 blended with 10 wt% TMPEOTA increased after a UV dose of 200 mJ/cm^2, and then decreased up to a UV dose of 1000 mJ/cm^2, and increased again, because 10 wt% TMPEOTA was almost cured, and a very tight network was formed. This tight network causes an increase in probe tack. The probe tack values of the PSA-A10 blended with TMPEOTA were maintained, due to the semi-IPN structure of TMPEOTA counterbalancing the plasticizer effect, as shown in Fig. 5b.

The probe tack values of the PSA-A15 and TMPEOTA blends decreased, as shown in Fig. 5c. However, the decrement of probe tack in the PSA-A15 and TMPEOTA blends is smaller than in PSA-A15 and TMPTA blends, because TMPEOTA has a longer chain length and a slower reactivity than TMPTA.

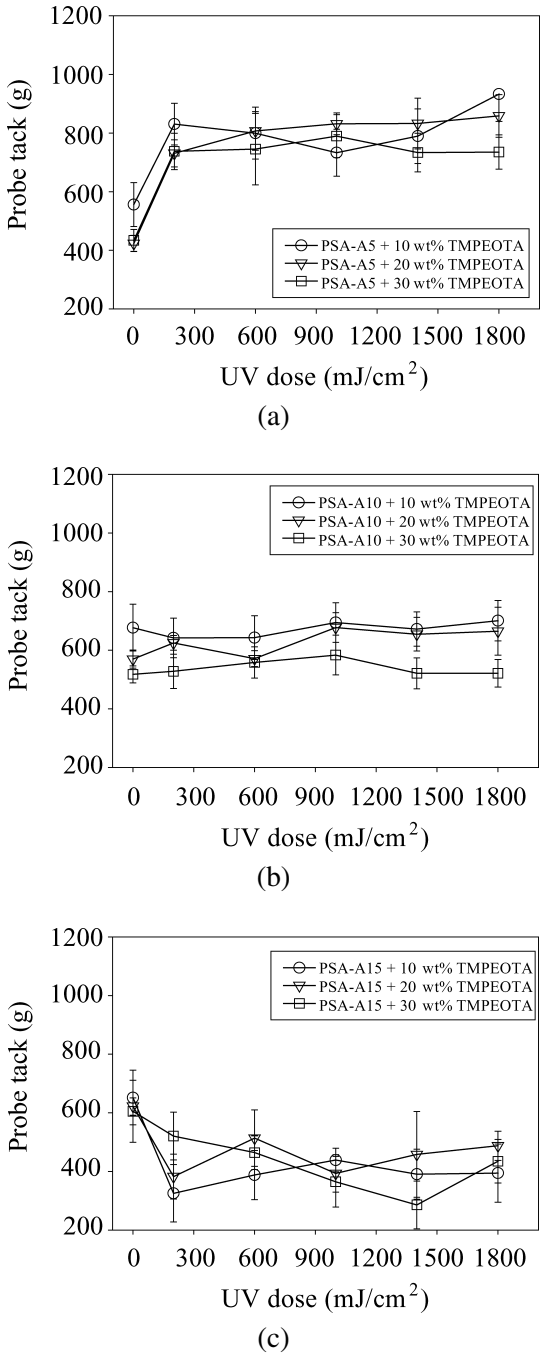

Figure 5. Probe tack of PSAs blended with (a) 10, (b) 20 and (c) 30 wt% TMPEOTA as a function of UV dose.

Overall, we observed that probe tack decreased with increasing AA concentration. Moreover, TMPTA had an effect on probe tack both before and after UV exposure, especially in PSA-A15 blended with TMPTA, because it has a low molecular weight and acts well as a plasticizer; however, TMPEOTA did not cause a significant change in probe tack before and after UV exposure because it also formed a more flexible crosslinked semi-IPN structure due to its long chain length after UV exposure.

3.2.3. Peel strength. The peel strength of the PSAs with TMPTA is shown in Fig. 6. The peel strength of the PSA-A5 and 10 wt% TMPTA blends increased until a UV dose of 1000 mJ/cm^2 because of the plasticizer effect of TMPTA, but the peel strength of the PSA-A5 and 10 wt% TMPTA blends decreased after a UV dose of 1000 mJ/cm^2 because the UV-cured TMPTA formed tightly crosslinked semi-IPN structure, restricting their mobility. For similar reasons, the 20 and 30 wt% blends of TMPTA with PSA-A5 showed reduced peel strength upon UV exposure, because of the tight network of TMPTA.

The PSA-A10 blended with TMPTA showed a decrease in peel strength after UV irradiation, as shown in Fig. 6b. One reason may be that the PSA-A10 has a higher T_g than the PSA-A5, and that the peel strength of the PSA-A10 and TMPTA blends is higher than that of the PSA-A5 and TMPTA blends. Another reason may be the tight network of TMPTA, which leads to low tack. PSA-A15 and TMPTA blends show results similar to the PSA-A10 and TMPTA blends, as shown in Fig. 6c. However, the PSA-A15 and TMPTA blends show a higher peel strength than the PSA-A10 and TMPTA blends, because PSA-A15 has the highest T_g among the three PSAs.

The peel strength of PSA-A5 blended with TMPEOTA did not change after UV irradiation, as shown in Fig. 7a. PSA-A5 has lower T_g and viscosity and a better mobility than the other two PSAs, and additionally, TMPEOTA has long chains. Therefore, their blend is soft after UV irradiation, and its peel strength is not changed upon UV irradiation. However, the PSA-A5 and TMPEOTA blends show a failure mode change from cohesive failure before UV exposure to the interfacial failure mode after UV exposure. In contrast, the peel strength of the PSA-A10 and TMPEOTA blends increased after UV exposure, as shown in Fig. 7b; before UV exposure, the PSA-A10 and TMPEOTA blends are soft and showed low peel strength values, but after UV exposure a tightly crosslinked semi-IPN structure formed between the linear PSA polymers and the UV-cured TMPEOTA, and the peel strength increased and then slightly decreased because of the high cohesion of the blend due to the more compact semi-IPN structure of TMPEOTA formed. The peel strength of the PSA-A15 and TMPEOTA blends dramatically increased after UV irradiation, as shown in Fig. 7c, because these blends have increased cohesion after UV irradiation. Therefore, their peel strength increased and their failure modes became interfacial. Specifically, the peel strength of the PSA-A15 blended with 30 wt% TMPEOTA dramatically increased after UV exposure, and

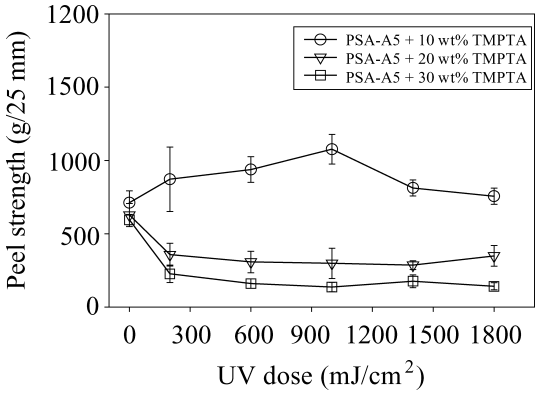

(a)

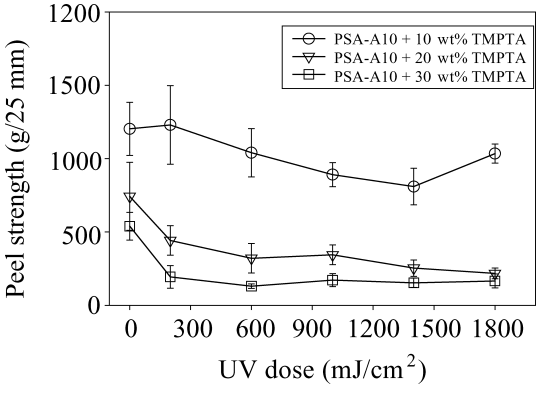

(b)

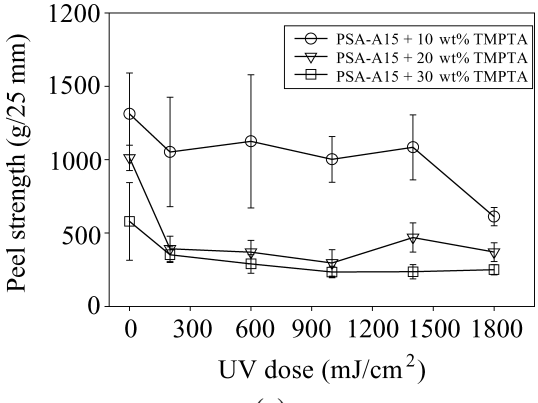

(c)

Figure 6. Peel strength of PSAs blended with (a) 10, (b) 20 and (c) 30 wt% TMPTA as a function of UV dose.

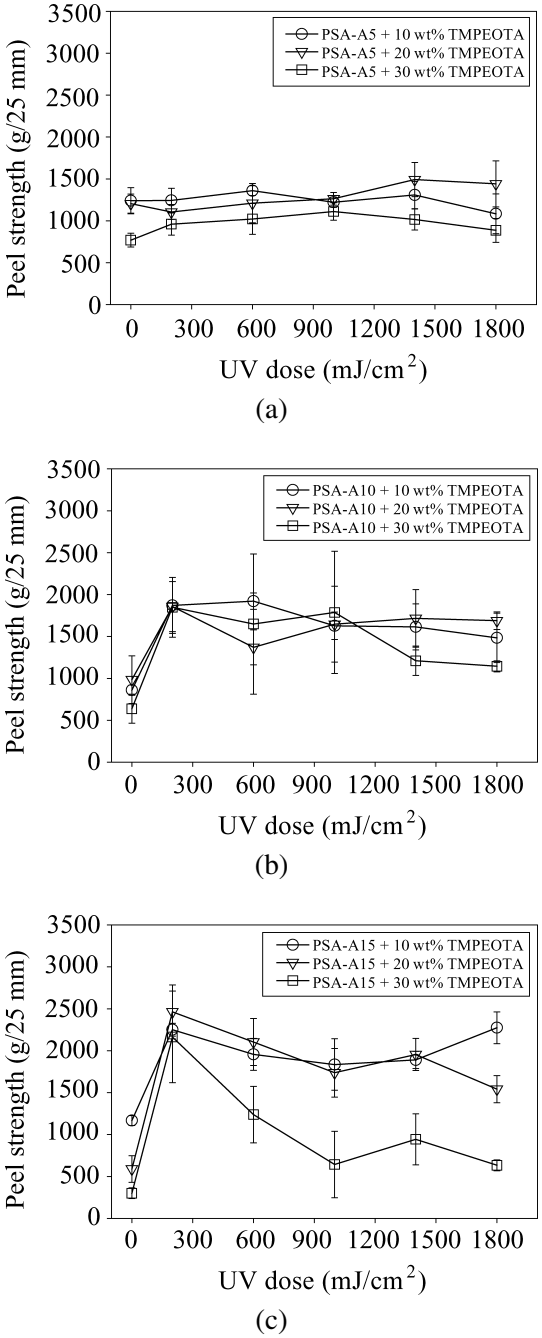

Figure 7. Peel strength of PSAs blended with (a) 10, (b) 20 and (c) 30 wt% TMPEOTA as a function of UV dose.

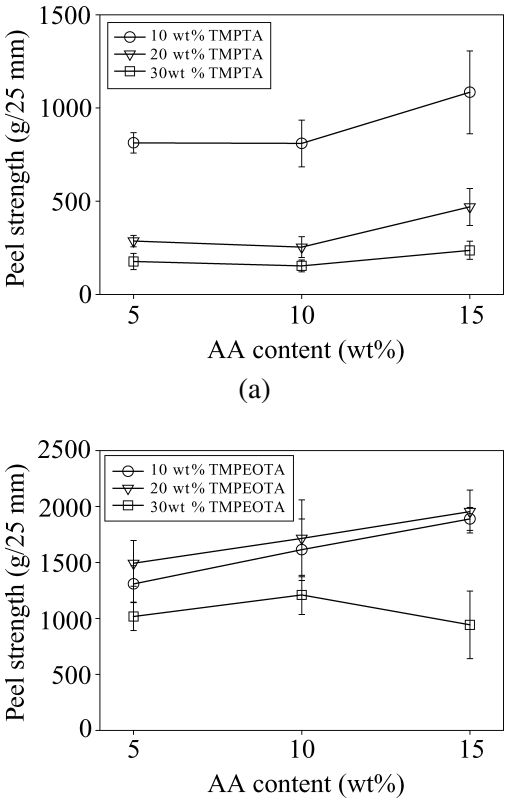

Figure 8. Peel strength of PSAs blended with (a) TMPTA and (b) TMPEOTA as a function of AA concentration at a UV dose of 1400 mJ/cm^2.

then highly decreased with additional UV exposure due to the existence of many reaction sites of TMPEOTA, which can form a tightly crosslinked structure.

From a different point of view, the peel strength increased with AA concentration, as shown in Fig. 8. The peel strength of the TMPTA blends decreased with increasing TMPTA content, because the short chain length of TMPTA causes tight crosslinking after UV exposure. The peel strength of the TMPTA blends clearly increased with AA concentration. The TMPEOTA blends showed results similar to the TMPTA blends. However, as TMPEOTA has a long chain length, so the cured TMPEOTA posesses mobility. This mobility can increase peel strength; therefore, the peel strength of 20 wt% TMPEOTA blend is higher than that of 10 wt% TMPEOTA blend. However, the peel strength of the 30 wt% TMPEOTA blend increased and then decreased with increasing UV exposure, because cured TMPEOTA can restrict the mobility of PSA-A15 and TMPEOTA.

3.2.4. SAFT. The SAFT can be measured as the heat resistance of a sample at elevated temperature under a constant force. In this study, SAFT could not

be measured over 150°C because of the temperature limitations of the equipment. Therefore, SAFT over 150°C is expressed as 150°C in the graph.

Figure 9 shows the SAFT of PSA-A5 blended with TMPTA. The PSA-A5 blended with TMPTA shows a dramatic increase in SAFT after UV exposure, and then appears to have a SAFT over 150°C after a UV dose of 600 mJ/cm^2. The SAFT of PSA-A5 blended with TMPTA at a UV dose of 200 mJ/cm^2 was carefully observed. The increased TMPTA content in the PSAs shows an increase in the SAFT because of similar reasons as mentioned above for probe tack and peel strength results.

The SAFT values of the PSA-A10 and TMPTA blends show results similar to the PSA-A5 with TMTPA blends, as shown in Fig. 9b. However, the PSA-A10 blended with TMPTA has a steeper slope than the PSA-A5 blended with TMTPA, i.e., at a UV dose of 200 mJ/cm^2, the SAFT of the PSA-A5 with TMPTA blends is about 50°C, but the SAFT of the PSA-A10 with TMPTA blends is about 80°C. The SAFT of the PSA-A15 and 10 wt% TMPTA blend steeply increased after UV exposure, and reached over 150°C after a UV dose of 200 mJ/cm^2. However, the PSA-A15 blended with 20 and 30 wt% of TMPTA showed SAFT values of about 90°C at a UV dose of 200 mJ/cm^2, and then the SAFT values reached over 150°C after prolonged UV irradiation. With the PSA-A15 and 10 wt% TMPTA blend, a SAFT of over 150°C was easy to reach, but the PSA-A15 and 20 or 30 wt% of TMPTA blends showed low slopes because of lumps of TMPTA formed.

Figure 10a shows the SAFT of the PSA-A5 and TMPEOTA blends. The PSA-A5 and 10 wt% TMPEOTA blend showed a high increment in the SAFT after UV exposure, and the SAFT reached over 150°C after a UV dose of 1400 mJ/cm^2, because it reacts more slowly than TMPTA. Moreover, the SAFT of the PSA-A5 and 20 wt% TMPEOTA blend increased and was maintained at about 40°C. The reason for this is that TMPEOTA posesses mobility, which makes PSA-A5 soft. Therefore, the SAFT of the PSA-A5 and 20 wt% TMPEOTA blend is lower than that of the PSA-A5 and 10 wt% TMPEOTA blend after UV exposure. However, the SAFT of the PSA-A5 and 30 wt% TMPEOTA blend is higher than that of the PSA-A5 and 20 wt% TMPEOTA blend after UV exposure because 30 wt% TMPEOTA formed more tightly crosslinked structure than 20 wt% TMPEOTA.

The SAFT of the PSA-A10 blended with TMPEOTA was similar to the SAFT of the PSA-A10 and TMTPA blends. PSA-A10 blends after UV exposure showed drastically increased SAFT results than PSA-A5 blends because PSA-A10 has a higher cohesion. In contrast, the SAFT of all PSA-A15 and TMPEOTA blends reached over 150°C after a UV dose of 200 mJ/cm^2. Therefore, the slopes of the PSA-A15 and TMPEOTA blends increase more steeply than those of the PSA-A10 and TMPEOTA blends because the T_g of PSA-A15 is higher than the T_g of PSA-A10. Also, the slope change of SAFT of the PSA-A15 blended with TMPEOTA was higher than that of SAFT of the PSA-A15 and TMPTA blends because TMPEOTA has a higher degree of freedom than TMPTA in PSA-A15. In addition, cured TMPEOTA does not form lumps.

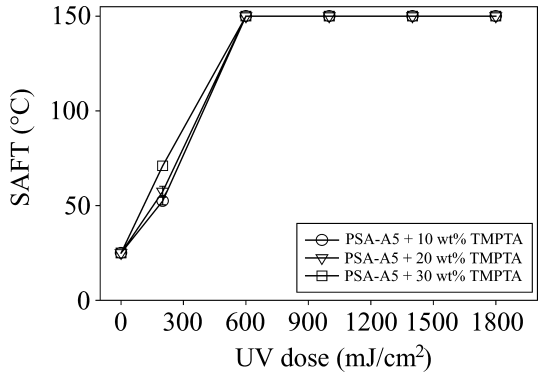

(a)

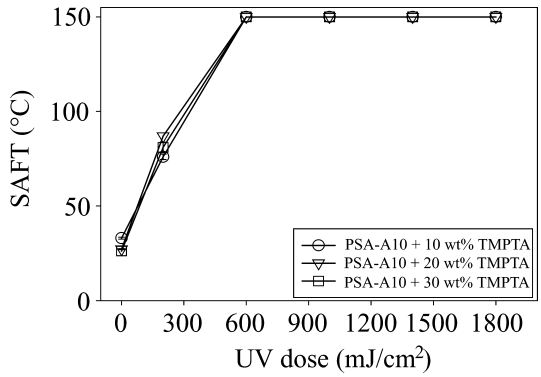

(b)

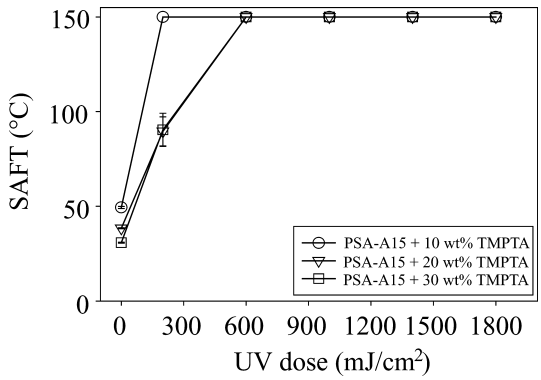

(c)

Figure 9. SAFT values of PSAs blended with (a) 10, (b) 20 and (c) 30 wt% TMPTA as a function of UV dose.

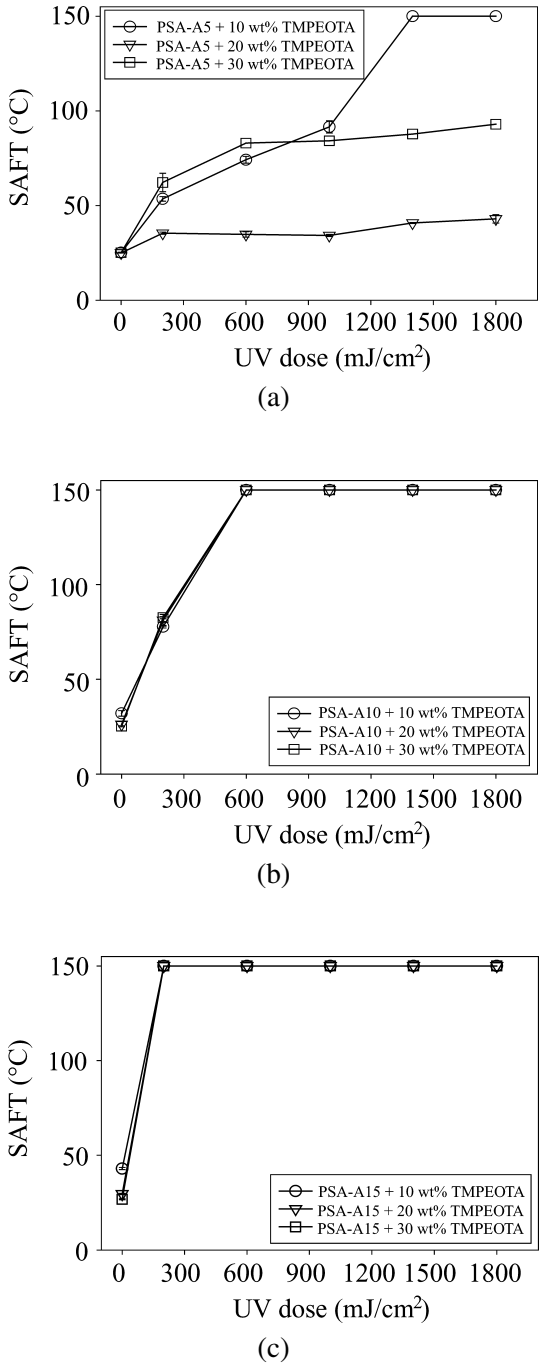

Figure 10. SAFT values of PSAs blended with (a) 10, (b) 20 and (c) 30 wt% TMPEOTA as a function of UV dose.

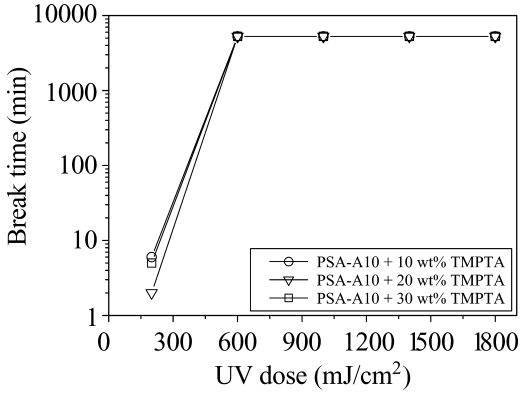

(a)

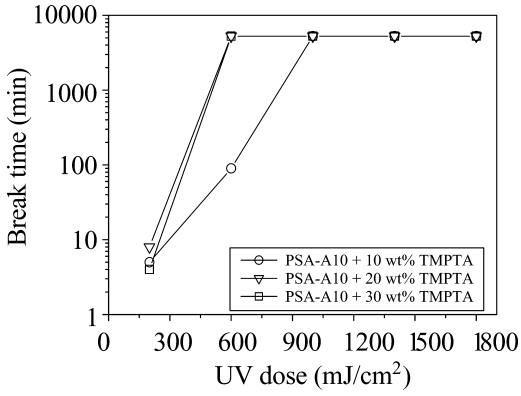

(b)

Figure 11. Holding power (in terms of break time) of PSAs blended with TMPTA (a) and TMPEOTA (b) as a function of UV dose.

Trifunctional monomers are crosslinked by UV exposure, and crosslinking plays a significant role in increasing the SAFT. Tobing and Klein [14] reported that shear holding power increased with increasing gel fraction. Therefore, a high SAFT or long duration of shear holding power is evidence of crosslinking. In this study, similar tendencies are shown, in that both the gel fraction and the SAFT increased with increasing T_g of PSAs.

3.2.5. Holding power. Figure 11 shows holding power results for the PSA-A10 blended with TMPTA and TMPEOTA. Similar to SAFT results, before UV irradiation holding power cannot be measured because very soft PSAs slip from the surface of stainless steel. After the UV dose of 200 mJ/cm^2, samples also slip over a very short time because of softness of PSAs. However, when the PSAs were more exposed to UV, in most cases the break time drastically increased because the trifunctional monomer created semi-IPN structures in PSAs and thus the extent

of crosslinking increased. Similarly, Sosson *et al.* [16] reported that when an adhesive was weakly crosslinked, it showed a fluid-like behavior, but for a highly crosslinked adhesive, highly increased shear stress was shown. Therefore, the increased crosslinking of linear structure acrylic PSAs with trifunctional monomers increases heat resistance because of increased crosslinking by semi-IPN structures.

4. CONCLUSIONS

In order to control the T_g of PSAs, PSAs were synthesized with different concentrations of AA and were investigated by measuring their adhesion performance. Next, for UV curing, the prepared PSAs were blended with trifunctional monomers having different chain lengths and investigated their adhesion performance. Blended PSAs formed semi-IPN structures after UV exposure.

As the AA concentration increased, the T_g of PSAs increased because of the higher T_g of AA. Also, their viscosities increased due to formation hydrogen bonds between the carboxyl groups of AA. Furthermore, both peel strength and SAFT increased with increasing AA concentration because hydrogen bonds increased their cohesion, but probe tack decreased. In addition, the failure mode changed from cohesive failure to interfacial failure with increasing AA concentration.

After UV exposure, gel fraction of the blended PSAs increased because crosslinking of trifunctional monomers formed semi-IPN structures in linear-structure PSAs. Therefore, their cohesion increased. Consequently, their peel strength and heat resistance (SAFT and holding power) increased, but probe tack decreased because of tightly crosslinked semi-IPN structures with increasing trifuctional monomers concentration. In most cases, cohesive failure changed to interfacial failure after UV exposure.

The molecular weight difference between TMPTA and TMPEOTA shows different tendencies in adhesion performance of UV-curable PSAs. TMPTA mainly influences the cohesion of PSAs. It confers PSAs more tightly crosslinked structures due to its short chain length. In contrast, TMPEOTA having a longer chain length affects the mobility of PSAs.

As a consequence, adhesion performance of PSAs is closely related to the T_g of PSAs, and the two types of trifunctional monomers show different adhesion performances because of difference in their molecular structures.

Acknowledgements

This work was supported by the Seoul R&BD Program and the Brain Korea 21 project.

REFERENCES

1. D. Satas, in: *Handbook of Pressure Sensitive Adhesive Technology*, D. Satas (Ed.), pp. 1–21. Satas & Associates, Warwick, RI (1999).

2. G. Auchter, O. Aydin and A. Zettl, in: *Handbook of Pressure Sensitive Adhesive Technology*, D. Satas (Ed.), pp. 444–514. Satas & Associates, Warwick, RI (1999).
3. Z. Czech, *Polym. Int.* **52**, 347 (2003).
4. Z. Czech, *Polym. Adv. Technol.* **15**, 539 (2004).
5. Z. Czech, *Int. J. Adhesion Adhesives* **24**, 503 (2004).
6. J. Asahara, N. Hori, A. Takemura and H. Ono, *J. Appl. Polym. Sci.* **87**, 1493 (2003).
7. Z. Czech, *Polym. Bull.* **52**, 283 (2004).
8. C. Decker, T. N. T. Viet, D. Decker and E. Weber-Koehl, *Polymer* **42**, 5531 (2001).
9. A. Zosel, in: *Advances in Pressure Sensitive Adhesive Technology — 1*, D. Satas (Ed.), pp. 92–195. Satas & Associates, Warwick, RI (1992).
10. Y. Li and J. C. T. Kwak, *Langmuir* **20**, 4859 (2004).
11. H.-J. Kim and H. Mizumachi, *J. Appl. Polym. Sci.* **57**, 175 (1995).
12. A. H. Shojaei, J. Paulson and S. Honary, *J. Control. Rel.* **67**, 223 (2000).
13. H. Lakrout, C. Creton, D. Ahn and K. R. Shull, *Macromolecules*, **34**, 7448 (2001).
14. S. D. Tobing and A. Klein, *J. Appl. Polym. Sci.*, **79**, 2230 (2001).
15. C. Creton, in: *Adhesion Science and Engineering, Vol.1: The Mechanics of Adhesion*, A. V. Pocius, D. A. Dillard and M. K. Chaudhury (Eds), pp. 535–577. Elsevier, Amsterdam (2002).
16. F. Sosson, A. Chateauminois and C. Creton, *J. Polym. Sci. Part B: Polym. Phys.* **43**, 3316 (2005).